Polymerization of L,L-Lactide Initiated by Aluminum Isopropoxide Trimer or Tetramer

Adam Kowalski, Andrzej Duda,* and Stanislaw Penczek

Department of Polymer Chemistry, Center of Molecular and Macromolecular Studies, Polish Academy of Sciences, Sienkiewicza 112, 90-363 Lodz, Poland

Received November 26, 1997; Revised Manuscript Received January 27, 1998

ABSTRACT: Kinetics of polymerization of L,L-lactide (LA) initiated with aluminum isopropoxide (Al(O^iPr)$_3$) trimer (A_3) or tetramer (A_4) was followed by polarimetry and by gel permeation chromatography (GPC). Results of the kinetic measurements show that A_3 and A_4 react with LA with different rates; namely, the $k_{i(A_3)}/k_{i(A_4)}$ ratios (where $k_{i(A_3)}$ and $k_{i(A_4)}$ denote the rate constants of initiation with A_3 and A_4, respectively) determined at 20, 50, 80 (THF solvent), and 120 °C (dioxane-1,4 solvent), are equal to 2.8 × 10^3, 8.0 × 10^2, 2.9 × 10^2, and 1.1 × 10^2, respectively. Direct observations of the A_3/LA and A_4/LA reacting mixtures by means of ^{13}C NMR spectroscopy confirm this large difference of A_3 and A_4 reactivities in their reactions with LA. Initiation with A_4 is slow enough to give polymerization that is less under control, in comparison with that initiated by A_3 alone. However, due to the relatively low rate of propagation, in comparison with that of the $A_4 \rightarrow A_3$ transformation, the apparent rates of LA polymerization initiated with A_3 or A_4 tend to converge, particularly at higher monomer conversion degrees (>90 mol %) and at higher temperatures, suggesting that also the less reactive A_4 is eventually transformed into the tris(macroalkoxide) ((...−C(O)CH(CH_3)O)$_3$Al) growing species *almost* completely. Molecular weight ($\bar{M}_n$), polydispersity index ($\bar{M}_w/\bar{M}_n$), and kinetic measurements of the A_3-initiated LA polymerization reveal a living character of this process: initiation is fast and quantitative, each −O^iPr group of A_3 starts growth of one macromolecule, and the concentration of the resulting active centers remains constant. On the other hand, propagation exhibits fractional order (e.g., equal to 0.7 at 80 °C in THF solvent) in active centers. Therefore, kinetic data were analyzed by assuming that the actually propagating active species (P_n*) aggregate reversibly into the unreactive dimers.

Introduction

High molecular weight poly(lactid acid) (PLA) is usually prepared by the ring-opening polymerization of the respective cyclic dimer—lactide (LA), i.e., L,L-LA, D,D-LA, (L,L + D,D)-LA, or L,D-LA.[1] Stannous octoate (tin(II) 2-ethylhexanoate, Sn(Oct)$_2$) is probably the most widely used initiator (catalyst?) for this purpose.[1−9] It looks, on the basis of our not yet published work,[10] that Sn(Oct)$_2$ is converted into the actual initiator in reaction with the −OH-containing compounds, either present adventitiously in the reaction mixture or purposely added, as was already suggested.[2,6,7] This view differs from the recently proposed mechanism,[8,9] in which Sn(Oct)$_2$ merely serves as an activator for monomer. However, the Sn(Oct)$_2$-promoted polymerization could hardly be controlled and its mechanism remains still obscure. Therefore, a variety of organometallic derivatives, particularly metal alkoxides, is continuously tested as initiators in the polymerization of lactides.[11−24]

The aluminum alkoxide initiators are the most versatile and readily available. Both monoalkoxides (R_2AlOR′)[11,13,15,17,21,24] and trialkoxides (Al(OR)$_3$)[12,14−16,20,23,24] were applied by several groups. In our opinion, the latter deserve attention, particularly now, when it becomes apparent that by using only one form of aluminum isopropoxide (Al(O^iPr)$_3$), namely its trimer, a perfect control of polymerization can be achieved.[25−27]

Polymerization of L,L- and (L,L + D,D)-LA, initiated with Al(O^iPr)$_3$ was claimed to be the first example of the fully controlled synthesis of high molecular weight PLA.[14,16] Moreover, according to our recent measurements,[23,24] the aluminum trialkoxide growing species belong to the most selective ones, in comparison with other metal (e.g., K, Sm, La, Fe, Sn, Ti) alkoxides.[24]

On the other hand, Al(O^iPr)$_3$ is known to exist in a form of a mixture of at least two aggregates, namely of a trimer (A_3) and a tetramer (A_4) (cf. A_3 and A_4 structures, R = CH(CH_3)$_2$).[28−32]

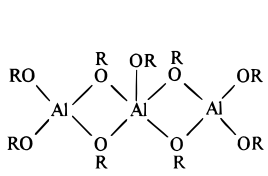

(A_3)

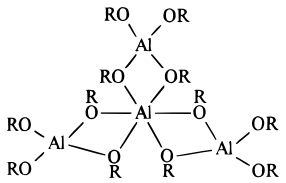

(A_4)

We have observed that the rate of $A_3 \rightleftharpoons A_4$ interconversions in C_6D_6 solvent, C_6D_6/ϵ-caprolactone (ϵCL), and THF/ϵCL solutions ([Al] ≤ 0.1 mol·L^{-1}) is slow, when compared with the rate of ϵCL propagation.[25,26] It was also revealed, by using ^1H NMR spectroscopy and kinetic measurements, that A_3 is much more reactive than A_4 in the reaction with ϵCL. From the initiator reacted with ϵCL, all three −O^iPr groups from Al(O^i-Pr)$_3$ are transferred into the poly(ϵCL) as the end groups. The resulting active species assumes mostly the nonaggregated (monomeric) three-arm structure: Al-{[−O(CH_2)$_5$C(O))]$_n$−OCH(CH_3)$_2$}$_3$, as determined by the multiangle laser light scattering (MALLS) and gel permeation chromatography (GPC) measurements of molecular weights of the living and the deactivated poly(ϵCL)'s, respectively.[26] These findings have been confirmed more recently by means of the ^1H NMR and viscosimetric analyses.[27]

S0024-9297(97)01737-3 CCC: $15.00
Published on Web 03/15/1998

Thus, when polymerization of ϵCL was initiated by an A_3/A_4 mixture (usually obtained for $Al(O^iPr)_3$ purified by the vacuum distillation), A_3 was consumed completely, whereas A_4 remained unreacted, at least within the time required for the complete ϵCL polymerization:

$$xA_3 + yA_4 + n\epsilon CL \rightarrow 3xAl\{[-O(CH_2)_5C(O)]_p-OCH(CH_3)_2\}_3 + yA_4 \quad (1)$$

$$n = \bar{p}\cdot x$$

In the polymerization of LA, consequences of the aggregation of $Al(O^iPr)_3$ initiator seemed to be less important[12,14,16,27] and this process was assumed to proceed in agreement with the net equation

$$xA_3 + yA_4 + nLA \rightarrow (3x + 4y)Al\{[-OCH(CH_3)C(O)]_p-OCH(CH_3)_2\}_3 \quad (2)$$

$$n = (3x + 4y)3\bar{p}$$

It may be due to the lower reactivity of the LA monomers, when compared with that of ϵCL. Thus, lactides may give A_4 enough time to rearrange into the reactive A_3 (or any other reactive form), and eventually both aggregates are consumed before polymerization is completed.

More detailed analysis of this system presented in the present work provides evidence that also in the case of polymerization of L,L-LA (denoted further as LA) initiation with A_4 is slow enough to give polymerization behavior that is less under control, in comparison with polymerization initiated by A_3 alone. The lower the temperature of polymerization, the more pronounced is the difference between kinetics and the overall control in polymerizations initiated with A_3 and A_4.

Experimental Section

Substrates and Solvents. L,L-Lactide (LA) (from Boehringer Ingelheim), crystallized consecutively from dry 2-propanol and toluene, was purified just before use by sublimation in vacuo (10^{-3} mbar, 85 °C) and distributed into the glass ampules equipped with breakseals.

Aluminum isopropoxide (from Aldrich) was purified by three consecutive distillations under reduced pressure (150 °C, 2 mbar) and stored at −12 °C, giving a mixture of a trimer (A_3) and a tetramer (A_4). A_3 was prepared starting from this A_3/A_4 mixture, according to the procedures given in ref 25. Namely, the aluminum isopropoxide distillate, sealed in the evacuated glass ampules, was placed in the oil bath at 150 °C for 2 h. The resulting melt was quenched in liquid nitrogen and then allowed to warm to room temperature, giving a viscous liquid composed (^{1}H NMR) mostly of A_3. A_3 was prepared also in the diluted dioxane-1,4 solutions (≈0.1 mol·L^{-1}) by thermostating the A_3/A_4 mixture at 110 °C for 48 h. A_4 was obtained using two different procedures. In one of these procedures, the A_3/A_4 mixture was dissolved in dry benzene (≈30 vol %) and then a 10-fold volume excess of the dry pyridine was added. The white solid precipitated out and the resulting supernatant was filtered off via the fritted glass. The remaining solid was additionally washed with dry pyridine and filtered off, and the residual pyridine was removed under vacuum (10^{-3} mbar at room temperature for several hours, until no more pyridine was detected by ^{1}H NMR). In the second approach, the liquid aluminum isopropoxide distillate (sealed in the evacuated glass ampules) was thermostated at 70 °C. Over several days the product gave a white polycrystalline solid. Both methods led to ^{1}H NMR pure tetrameric aluminum isopropoxide (A_4).

THF and dioxane-1,4 (from POCh Gliwice) were kept, after the usual purification, over liquid Na−K alloy, from which they were distilled in vacuo into the reaction vessel.

Polymerization Procedures. Polymerizing mixtures were prepared in sealed glass ampules using a standard high-vacuum technique.

Determination of the LA Conversion. Conversion (α) of LA was determined using both gel permeation chromatography (GPC) and polarimetry. GPC analyses were performed using an LKB 2150 HPLC pump and a set of Waters Ultrastyragel (10^3, 5×10^2, 10^2, 10^2) columns. A Wyatt Optilab 903 interferometric refractometer (from Wyatt Technology Corp.) was applied as the detector. THF was used as the eluent.

To determine the actual proportions of PLA and LA in the sample, the surface area under the monomer signal was multiplied by the correction factor (f_1) equal to 0.89. This value results from the ratio of the refractive index increments (dn/dc) determined by us for LA (0.0625 mL/g) and for PLA (0.0558 mL/g) in THF as a solvent. A similar f_1 value was obtained from direct measurements of the surface areas under the signals due to PLA and LA for the polymer/monomer mixtures of known composition.

Simultaneously, the LA monomer conversion was followed by a Perkin-Elmer 241 MC polarimeter. The living polymerization mixtures were prepared and transferred into the optical cells under the high-vacuum conditions and then sealed off. The optical rotations of the living polymerization mixtures (r) were measured at 578 nm at room temperature. The instantaneous monomer concentrations were determined by assuming additivity of the optical rotations for LA (r_m) and PLA (r_p), i.e., $[LA] = [LA]_0(r - r_p)/(r_m - r_p)$.

Determination of Molecular Weights ($\bar{M}_n$) and of Polydispersity Indexes ($\bar{M}_w/\bar{M}_n$). The actual number-average molecular weights ($\bar{M}_n$) of PLA were determined using the calibration method described already by us for poly(ϵ-caprolactone).[33] It was established, however, that in order to get the correct $\bar{M}_n$ value of PLA the experimental value, obtained from the GPC traces using polystyrene standards, have to be multipled by 0.58 (at least up to $\bar{M}_n \approx 10^4$). The actual number-average molecular weights ($\bar{M}_n$) of the deactivated and isolated PLA were measured on a Knauer vapor pressure osmometer in dry methylene chloride. The resulting $\bar{M}_n$ values were then used for GPC calibration. The $\bar{M}_w/\bar{M}_n$ ratios were determined directly from the GPC traces.

Preparation of Samples for GPC and $\bar{M}_n$ Measurements. GPC measurements were performed for the polymerizing mixtures deactivated with acetic acid. In another approach, polymerizing mixtures were dissolved in benzene, deactivated by washing three times with diluted HCl_{aq} and then with distilled water, until a pH of ≈7 was reached. After separation of the organic (benzene) and aqueous layers, the benzene solution of the polymer was lyophilized under reduced pressure and the unreacted monomer was sublimed out. Samples prepared in this way were used in osmometric and GPC measurements. Both methods of deactivation, i.e., with acetic acid and with HCl_{aq} led to the practically identical results from the GPC measurements.

NMR Measurements. ^{13}C NMR spectra were recorded in benzene-d_6 solvent or in the 85/15 (v/v) mixture of dioxane-1,4/benzene-d_6 on a Bruker AC200 apparatus operating at 50.33 MHz. Benzene was used as an internal standard (δ = 128.68 ppm). The reacting mixtures were prepared and transferred into the NMR tubes under high-vacuum conditions. The NMR tubes were eventually sealed off after freezing their contents with liquid nitrogen.

Results and Discussion

^{13}C NMR Studies. In the previous works,[25,26] concerning polymerization of ϵ-caprolactone (ϵCL) initiated with A_3 and A_4, we applied ^{1}H NMR spectroscopy to determine structures of the initiators, the resulting active centers, and end-groups. Particularly useful was

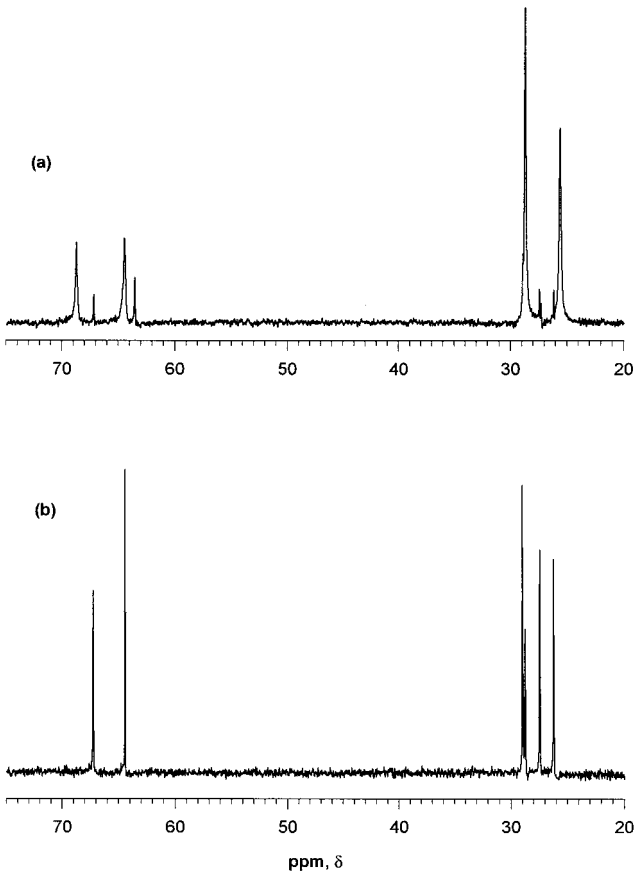

Figure 1. $^{13}C\{^1H\}$ NMR (50.33 MHz) spectra of 98% trimeric $Al(O^iPr)_3$ (A_3) (a) and of tetrameric $Al(O^iPr)_3$ (A_4) (b). Conditions of measurement: $[Al(O^iPr)_3] = 0.1$ mol·L^{-1}, benzene-d_6 as a solvent, 23 °C.

the methine protons absorption range. The LA monomer contains methine protons itself, giving strong signals overlapping with those of the end groups. Therefore, in the present work, we decided to use ^{13}C NMR spectroscopy, which allowed detection of initiator in the presence of LA. The best results were obtained for the methyl groups (CH_3) absorption range.

(a) ^{13}C NMR Spectra of a Trimer $(Al(O^iPr)_3)_3$ (A_3) and of a Tetramer $(Al(O^iPr)_3)_4$ (A_4). Figure 1 shows the $^{13}C\{^1H\}$ NMR spectra of $Al(CH(CH_3)_2)_3$ trimer (A_3) (a) and tetramer (A_4) (b) recorded in C_6D_6 as a solvent. In the spectrum of A_3 (Figure 1a) there are two dominating groups of the relatively broad signals: corresponding to the methine carbon atoms at $\delta = 68.75$ and 64.50 ppm and to the methyl carbon atoms at $\delta =$ 28.74 and 25.66 ppm. Purity of A_3 is about 98 mol %, according to the ^1H NMR spectra;[25] the remaining signals of the apparently lower intensity are due to the ≈2 mol % admixture of A_4 (the respective chemical shifts are given below). For signals in the spectrum of A_4 (Figure 1b) the following assignment have already been made:[34] $\delta = 67.28$ and 64.45 ppm due to the methine carbon atoms in the bridge and the external isopropoxy groups; two pairs at $\delta = 29.04$ and 28.80 ppm and at δ = 27.52 and 26.29 ppm due to the methyl carbon atoms in the external and bridge (axial and equatorial) isopropoxy groups, respectively.

(b) Comparison of Reactivities of A_3 and of A_4 in Polymerization of L,L-Lactide. The reaction of A_3 with LA at room temperature gives, soon after mixing of the substrates, the first addition products, according

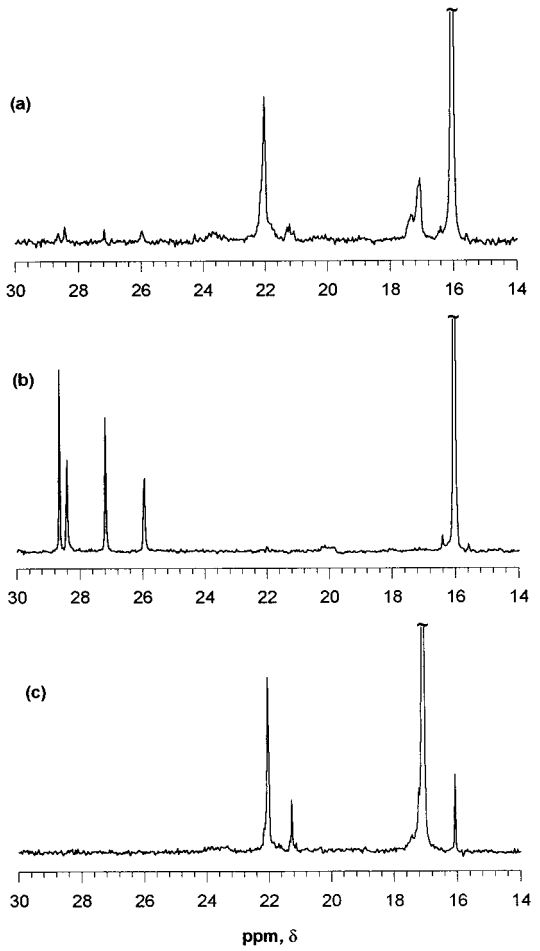

Figure 2. Methyl group absorption range of the $^{13}C\{^1H\}$ NMR (50.33 MHz) spectra (of A_3/l,l-lactide (a), of A_4/L,L-lactide (b) reacting mixtures recorded after mixing reagents at 20 °C, and of the living poly(L,L-lactide) (c)). Conditions: $[Al(O^iPr)_3]_0 =$ 0.1 mol·L^{-1}, $[LA]_0 = 1.0$ mol·L^{-1}, dioxane-1,4/benzene-d_6 (90/10 v/v) as a solvent.

to the equation

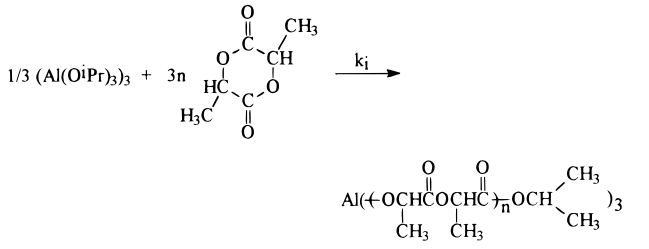

(3)

This is illustrated in the ^{13}C NMR spectrum of the A_3/LA reaction mixture (Figure 2a), showing no signals corresponding to A_3, which apparently was quantitatively consumed. The peak at $\delta = 22.01$ ppm can be ascribed to the $(CH_3)_2CHO-C(O)CH(CH_3)O-...$ end group,[11] and the signal centered at $\delta = 17.06$ ppm, to the first two lactidiyl units: $(CH_3)_2CHO-C(O)CH-(CH_3)O-C(O)CH(CH_3)O-Al<$ inserted into the aluminum−oxygen bond of the initiator. The sharp peak at $\delta = 16.01$ ppm, dominating in the spectrum, comes from the LA monomer, which remains at this stage largely unreacted.

The small signals at $\delta = 21.21$ and 23.68 ppm are related probably to the small fraction of the addition

products with one or two unreacted $-O^iPr$ groups at one Al atom and/or to the nonaggregated aluminum tris(macroalkoxide) growing species (cf. last section of the present paper). Four small peaks in the range from $\delta = 28.63$ to 25.95 ppm correspond to the unreacted A_4.

In contrast, A_4 in the mixture with LA, under otherwise identical conditions, remains practically intact, as shown in the respective ^{13}C NMR spectrum (Figure 2b) in which the signals due to A_4 and LA are exclusively present (at $\delta = 28.62$, 28.39, 27.16, and 25.94 ppm, and at $\delta = 16.00$ ppm, respectively).

Only after a longer time and at a higher temperature (e.g., 24 h, 80 °C) do both A_3/LA and A_4/LA reaction mixtures give practically identical ^{13}C NMR spectra (Figure 2c), containing absorption bands of $(CH_3)_2CHO-C(O)CH(CH_3)O-$... end groups at $\delta = 22.00$ ppm, the PLA lactidiyl $(CH_3)_2CHO-[C(O)CH(CH_3)O]_n-Al<$ repeating units at $\delta = 17.03$ ppm, and the unreacted LA monomer, present at equilibrium concentration (0.055 mol·L^{-1} at 80 °C; cf. ref 4) at $\delta = 16.0$ ppm.

Concluding, we observed directly, by means of the ^{13}C NMR spectroscopy, that A_3, like in the polymerization of ϵ-caprolactone (ϵCL),[25,26] also initiates polymerization of LA considerably faster than A_4 does. Determination of the respective rate constants, and their comparison with those reported in the previous paper on the ϵCL polymerization,[26] will be described in the last two sections of this paper, discussing kinetics of the LA polymerization.

Dependence of PLA Molecular Weights and Their Distribution on the Aggregation Form (A_3 or A_4) of the Al(O^{i}Pr)$_3$ Initiator. Polymerization of LA initiated with A_3 or A_4, carried out in THF as a solvent in the temperature range from 20 to 80 °C and at 120 °C in dioxane-1,4 was studied more systematically. The starting concentrations of LA ($[LA]_0$) and initiators—in terms of the Al(O^{i}Pr)$_3$ units ($[Al]_0$)—were equal, in all experiments reported in the present section, to 1 and 0.01 mol·L^{-1}, respectively. An aim of the present work was not to optimize the high molecular weight PLA synthesis, but only to study differences in A_3 and A_4 kinetic behavior, so the applied $[Al]_0$ was relatively high (and, consequently, the resulting $\bar{M}_n$ relatively low) in order to obtain operable polymerization times, particularly at lower temperatures.

Results of measurements of the number average molecular weights ($\bar{M}_n$) and of polydispersity indexes ($\bar{M}_w/\bar{M}_n$) (both by GPC, cf. Experimental Section) at various degrees of monomer conversion ($\alpha = ([LA]_0 - [LA])/[LA]_0$) and temperatures are collected in Figures 3 and 4. The solid lines in Figure 3 show dependencies of $\bar{M}_n$ on α, calculated with an assumption that each isopropoxide group of the $(Al(O^iPr)_3)_x$ ($x = 3$ or 4) initiator starts growth of the only one PLA macromolecular chain, in agreement with

$$(1/x)(Al(O^iPr)_3)_x + 3n\,LA \rightarrow Al((OCH(CH_3)C(O))_{2n}-O^iPr)_3$$

$$Al((OCH(CH_3)C(O))_{2n}-O^iPr)_3 \xrightarrow{\text{hydrolysis}} 3H(OCH(CH_3)C(O))_{2n}-O^iPr \quad (4)$$

i.e.

$$\bar{M}_n(\text{calc}) = 144.13\alpha[LA]_0/3[Al]_0 + 60.10 \quad (5)$$

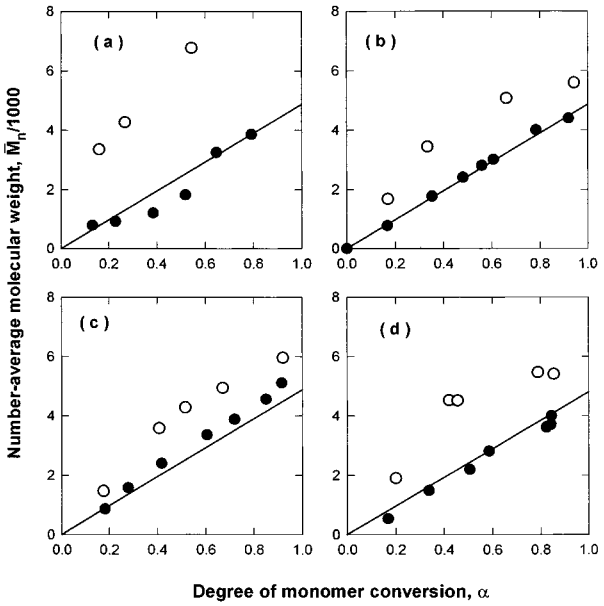

Figure 3. Dependence of the number-average molecular weight ($\bar{M}_n$) on the monomer conversion degree ($\alpha = ([LA]_0 - [LA])/[LA]_0$) in the polymerization of L,L-lactide initiated with A_3 (●) or A_4 (○). Polymerization conditions $[LA]_0 = 1$ mol·L^{-1}, $[Al(O^iPr)_3]_0 = 0.01$ mol·L^{-1}, temperature (in °C) = 20 (a), 50 (b), 80 (c) (THF solvent), 120 (d) (dioxane-1,4 solvent). Lines were calculated by assuming the absence of transfer (cf. eq 6).

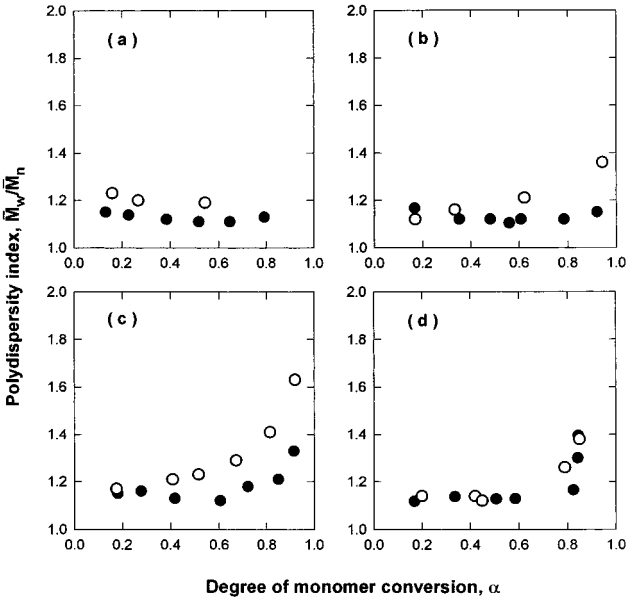

Figure 4. Dependence of the polydispersity index ($\bar{M}_w/\bar{M}_n$) on the monomer conversion degree ($\alpha = ([LA]_0 - [LA])/[LA]_0$) in the polymerization of L,L-lactide initiated with A_3 (●) or A_4 (○). Polymerization conditions are given in the caption for Figure 3.

where 144.13 and 60.10 are the molecular weights of the dilactydiyl repeating unit and of the introduced end groups (H− and $-O^iPr$), respectively; $[Al]_0 = x[(Al(O^iPr)_3)_x]_0$.

For the initiation with A_3 the calculated and experimentally determined dependencies of $\bar{M}_n$ on α are close to each other, within the estimated experimental error, indicating a quantitative initiation and an absence of the transfer side reaction, leading to the uncontrolled increase of the number of growing macromolecules.

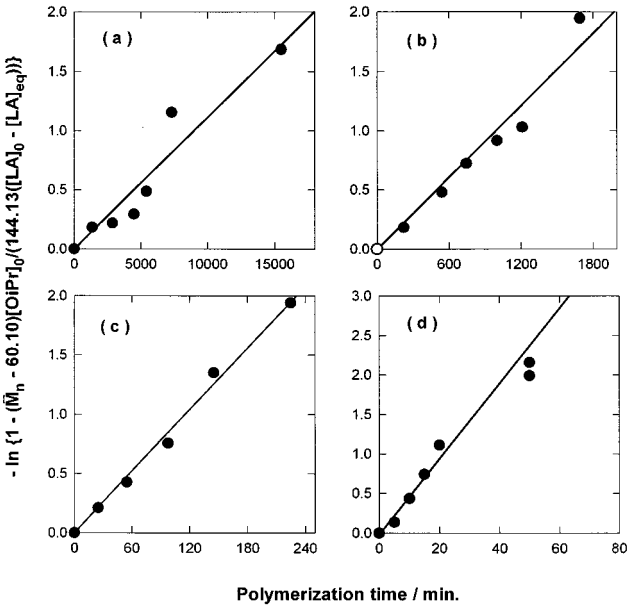

Figure 5. Dependence of $\ln\{1 - ((\bar{M}_n - 60.10)/144.13)/(([LA]_0 - [LA]_{eq})/[O^iPr]_0)\}$ on time (eq 6) as a criterion of the livingness[35] of the L,L-lactide polymerization initiated with $Al(O^iPr)_3$ trimer (A_3). Polymerization conditions are given in the caption for Figure 3.

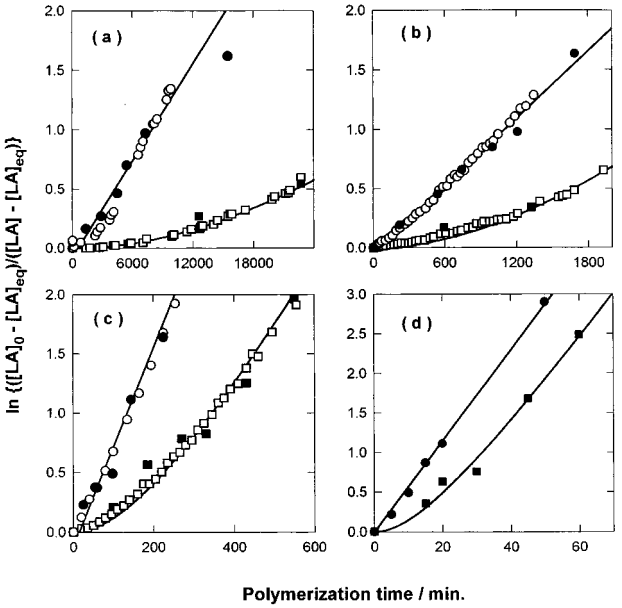

Figure 6. Kinetics of L,L-lactide (LA) polymerization initiated with $Al(O^iPr)_3$ trimer (A_3) or tetramer (A_4). Polymerization conditions are given in the caption for Figure 3. Experimental points: (○) A_3, polarimetry; (●) A_3, GPC; (□) A_4, polarimetry; (■) A_4, GPC. Lines were obtained from the straight linear regression of the experimental data (A_3) or from the numerical curve fitting, according to the integrated equations (10) (A_4).

Moreover, an analysis of evolution of $\bar{M}_n$ with polymerization time (t), in terms of the diagnostic criterion of the livingness of polymerization elaborated recently in our laboratory,[35] i.e., correlation of $\bar{M}_n$, $[O^iPr]_0$, and t by means of the formula

$$-\ln\left(1 - \frac{(\bar{M}_n - 60.10)/144.13}{([LA]_0 - [LA]_{eq})/[O^iPr]_0}\right) = k_p[O^iPr]_0 t \quad (6)$$

(where $[LA]_{eq}$ is the LA monomer concentration at equilibrium), shows (Figure 5) that not only transfer but also termination is practically eliminated in the A_3 initiated polymerization of the LA monomer.

For the initiation with A_4, the experimental $\bar{M}_n$ values exceed considerably, at least at the lower LA conversion, those calculated by assuming a living polymerization mechanism, showing that indeed initiation is slow when compared with propagation. For the conversion degrees approaching $\alpha_{eq} = ([LA]_0 - [LA]_{eq})/[LA]_0$ the actual $\bar{M}_n$'s tend to approach those predicted by formula 5, indicating that A_4 is consumed almost quantitatively when the polymerization is completed.

Polydispersity indexes ($\bar{M}_w/\bar{M}_n$), being a measure of molecular weight distribution (MWD), are slightly higher for PLA's prepared with A_4, whatever is the monomer conversion and polymerization temperature (at least for $\alpha < \alpha_{eq}$ and excepting 120 °C) (Figure 4), which again may be attributed to the slow initiation.

It has to be stressed that even for A_3, initiating fast and quantitatively, the resulting $\bar{M}_w/\bar{M}_n$ are higher than expected for the living polymerization (i.e. $\bar{M}_w/\bar{M}_n \approx 1$) and, moreover, their values increase with conversion.

The latter phenomenon can be related to the transesterification side reactions, inevitably accompanying polymerization of cyclic esters. In the particular case of lactides, this is mostly the intermolecular reaction, not changing $\bar{M}_n$ but broadening MWD (i.e., increasing $\bar{M}_w/\bar{M}_n$), e.g.

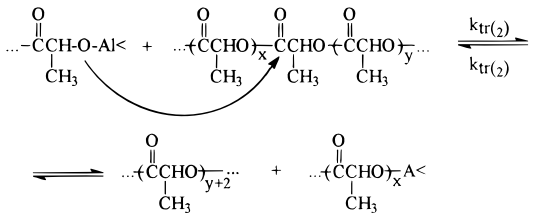

(7)

where $k_{tr(2)}$ denotes the rate constant of the intermolecular (bimolecular) transesterification.

In our recent publications[24,25] we analyzed this phenomenon in more detail and showed how to determine the ratio of the rate constant of propagation to that of intermolecular transesterification ($k_p/k_{tr(2)}$) by adjusting the numerically simulated plots of $\bar{M}_w/\bar{M}_n$ as a function of α to the experimental data. For the polymerization of L,L-lactide with the aluminum trialkoxide active centers (initiation by A_3) the value of $k_p/k_{tr(2)}$ is equal to 10^2 (THF, 80 °C).

Comparison of Kinetics of L,L-Lactide Polymerizations Initiated with $Al(O^iPr)_3$ Trimer or Tetramer. Polymerization of LA initiated with A_3 or A_4, conducted in THF solvent in the temperature range from 20 to 80 °C and at 120 °C in dioxane-1,4, was studied polarimetrically and chromatographically (GPC). The starting concentrations of LA and of $Al(O^iPr)_3$ in all kinetic experiments were equal to 1 and to 0.01 mol·L^{-1}, respectively. Results of the kinetic measurements are given in Figure 6 in the semilogarithmic coordinates: $\ln\{([LA]_0 - [LA]_{eq})/([LA] - [LA]_{eq})\}$ versus time.

According to our earlier measurements,[4] carried out in dioxane-1,4 solvent, $[LA]_{eq}$ increases from 0.01 to 0.15 mol·L^{-1} in the temperature range from 20 to 130 °C (in THF as a solvent practically identical $[LA]_{eq}$ values were

Table 1. Comparison of Kinetic Parameters Characterizing Polymerizations of ϵ-caprolactone and L,L-Lactide Initiated with A_3 and A_4[a]

	monomer				
	ϵ-caprolactone	L,L-lactide			
temp/°C	20	20	50	80	120
k_p/mol^{-1}·L·s^{-1}	0.5	7.5×10^{-5}	5.5×10^{-4}	4.7×10^{-3}	3.2×10^{-2}
$k_{i(A_4)}$/mol^{-1}·L^{-1}·s^{-1}	5×10^{-6}	2.7×10^{-8}	6.9×10^{-7}	1.6×10^{-5}	2.9×10^{-4}
$k_{i(A_3)}/k_{i(A_4)}$	10^5	4.1×10^3	8.0×10^2	2.9×10^2	1.1×10^2

[a] Conditions of polymerization: (concentrations in mol^{-1}·L) $[\epsilon CL]_0 = 2$, $[LA]_0 = 1$, $3[A_3]_0 = 4[A_4]_0 = [Al(O^iPr)_3]_0 = 0.01$, THF solvent (at 120 °C, dioxane-1,4 solvent).

obtained, at least up to 90 °C). Thus, particularly at higher temperatures (usually used in lactide polymerization) and for higher monomer conversions, the value of $[LA]_{eq}$ has to be taken into account in the analysis of the kinetic data.

As seen in Figure 6, polarimetry and GPC give practically identical kinetic plots; this result proves indirectly that racemization in the LA/Al(O^{i}Pr)$_3$ system plays, if anything, a minor role. Therefore, polarimetry appears to be a very convenient method for the continuous monitoring of L,L-lactide concentration, at least in the present polymerizing system.

Inspection in Figures 6a−d reveals that A_3 provides kinetic plots that are internally first-order in monomer from the very beginning of polymerization, whereas for A_4 the picture typical for slow initiation is observed. However, for higher degrees of monomer conversion, the propagation rate in the polymerization initiated with A_4 eventually approaches the value observed for the A_3 initiation. This is more apparent at higher polymerization temperatures. This behavior suggests that also the less reactive A_4 is eventually transformed into the growing species almost completely.

To estimate a ratio of the rates of initiation of LA polymerization with A_3 and A_4, under the otherwise identical conditions, we analyzed the kinetics of LA polymerization in terms of the formal kinetic scheme (8),

$$\begin{gathered} I + LA \xrightarrow{k_i} P_1^* \\ P_1^* + LA \underset{k_d}{\overset{k_p}{\rightleftharpoons}} P_2^* \\ \hline P_i^* + LA \underset{k_d}{\overset{k_p}{\rightleftharpoons}} P_{i+1}^* \\ \hline [I]_0 = [I] + [P_n^*] \end{gathered} \tag{8}$$

in which initiation is the net reaction, including all elementary steps from the aggregate (A_3 or A_4) to the first propagating species, where I stands for the initiator (A_3 or A_4), P_i^* stands for the growing species with the polymerization degree equal to i (>Al−(OCH(CH$_3$)-C(O))$_{2i}$−O^{i}Pr), and $[P_n^*] = \sum[P_i^*]$; k_i, k_p, and k_d are the respective apparent rate constants.

In the case of A_3, initiation is fast and quantitative, and we additionally assumed that $k_{i(A_3)} = k_p$. Then, the kinetics of the LA monomer consumption is described by the first-order equation

$$\ln\{([LA]_0 - [LA]_{eq})/([LA] - [LA]_{eq})\} = k_p^{app}[P_n^*]t \tag{9}$$

where $[P_n^*] = 9[A_3]_0 = 3[Al(O^iPr)_3]_0$ and t is the polymerization time. The apparent propagation rate constants (k_p^{app}), determined directly from slopes of the semilogarithmic anamorphoses of the kinetic plots in Figure 6 are given in Table 1.

In further analysis we assumed that these k_p^{app}'s are also valid for the LA polymerization initiated with A_4 since for both the A_3 and A_4 initiation the identical propagating species are eventually observed. In the latter case, the set of pertinent differential equations reads

$$\begin{aligned} -\frac{d[I]}{dt} &= k_{i(A_4)}[I][LA] \\ -\frac{d[LA]}{dt} &= k_{i(A_4)}[I][LA] + k_p([I]_0 - [I])([LA] - [LA]_{eq}) \end{aligned} \tag{10}$$

(where k_p stands for k_p^{app}).

Although there is a possibility of finding k_i and k_p by a trial-and-error method[36] we solved these kinetic equations by numerical integration using the EPISODE procedure.[37] The value of $k_{i(A_4)}$ has been adjusted by the nonlinear least squares minimization, until the best fit between the experimental and simulated kinetic curves was obtained. The numerical calculations have been performed using the Scientist (MicroMath) program. The resulting values of $k_{i(A_4)}$ and $k_{i(A_3)}/k_{i(A_4)}$ are collected in Table 1, and curves in Figure 6 are plotted according to the integrated equations (10).

In our previous works,[25,26] concerning polymerization of ϵ-caprolactone (ϵCL) initiated with A_3 and A_4, we have estimated the limit of the $k_{i(A_3)}/k_{i(A_4)}$ ratio as equal to $\approx 10^3$. This rather rough estimation was done on the basis of the polymerization times giving the same ϵCL conversion degree and on the quantity of the initiator consumed (the latter was calculated from $\bar{M}_n$ of the PCL) formed). Therefore, to compare ϵCL and LA polymerizations, in the present paper we decided to recalculate this $k_{i(A_3)}/k_{i(A_4)}$ value using the approach based on the kinetic equations (10). Results of these calculations are given also in Table 1.

As seen from the data in Table 1, k_p(LA)/k_p(ϵCL) is equal to $1.5 \cdot 10^{-4}$ at 20° in THF solvent. The difference of the apparent reactivities between A_3 and A_4 is much less pronounced for the less reactive ("slower") monomer (i.e. LA). Moreover, the higher is the polymerization temperature, the lower is the $k_p/k_{i(A_4)}$ ($\leq k_{i(A_3)}/k_{i(A_4)}$) ratio. This is a result of the higher temperature coefficient ("activation energy") for a slower reaction. Such kinetic behavior causes, at elevated temperatures the $k_p/k_{i(A_4)}$ ratio to be sufficiently low to allow the A_4 initiator to be reacted almost quantitatively before the polymerization is completed.

Thus, it seems that at the conditions usually applied in the LA polymerization, the molecular weight ($\bar{M}_n$) of PLA could be controlled to a certain extent by the ($[LA]_0$

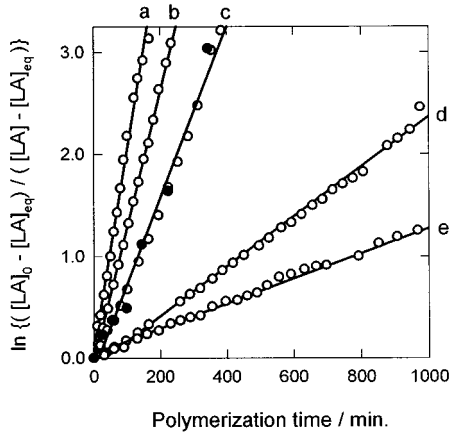

Figure 7. Kinetics of LA polymerization initiated with A_3 (○) polarimetry, (●) GPC). Polymerization conditions: $[LA]_0 = 1$ mol·L^{-1}, THF solvent, 80 °C; $[Al(O^iPr)_3]_0/(mol\cdot L^{-1}) = 5.3 \times 10^{-2}$ (a), 2×10^{-2} (b), 10^{-2} (c), 2.65×10^{-3} (d), 8.7×10^{-4} (e).

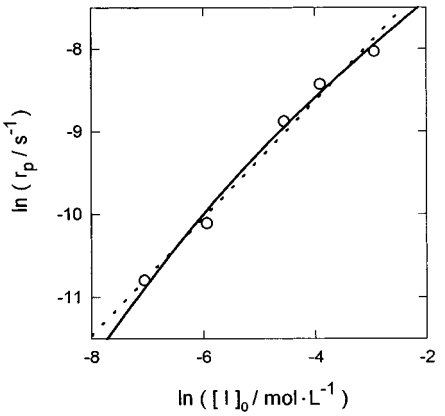

Figure 8. Plot of the order in initiator for the LA polymerization initiated with A_3. Polymerization conditions are as in the caption for Figure 7 ($r_p = (\ln\{([LA]_0 - [LA]_{eq})/([LA] - [LA]_{eq})\})/t$, $[I]_0 = [Al(O^iPr)_3]_0$). Dotted line: straight linear regression of the experimental points. Solid line: plot of $\ln r_p$ versus $\ln [I]_0$ computed on the basis of the kinetic scheme (11) assuming $m = 2$, $k_p = 8.2 \times 10^{-3}$ mol^{-1}·L·s^{-1}, and $K_a = 94$ mol^{-1}·L (eq 13).

$- [LA])/[Al(O^iPr)_3]_0$ ratio, even with the less reactive A_4, but only at the high monomer conversion and at higher temperatures. This conclusion is in agreement with results of the molecular weight measurements discussed in the preceding section.

Kinetics of L,L-Lactide Polymerization Initiated with A_3. Polymerization of LA initiated with A_3 looks like a living process. Indeed, the first-order kinetic plots (Figure 7), obtained for starting concentrations of Al-$(O^iPr)_3$ from 8.7×10^{-4} to 5.3×10^{-2} mol·L^{-1}, show no deviation from the straight linearity from the very beginning of the polymerization to at least 95 mol % of the monomer conversion (cf. also eq 6 and Figure 5).

Determination of the absolute rate constants of propagation is, however, not straightforward. The apparent rate constants of propagation ($k_p^{app} = -d[LA]/([LA]\cdot[I]_0)\, dt$), determined at 80 °C in THF solvent, increase from 2×10^{-3} to 7.9×10^{-3} mol^{-1}·L·s^{-1} for concentrations of active species decreasing from 5.3×10^{-2} to 8.7×10^{-4} mol·L^{-1}. A plot of the order in initiator (viz. active species—as confirmed by the $\bar{M}_n$ measurements) exhibits slope of 0.7 (dotted line in Figure 8). Such kinetic behavior could, for example, be explained by the reversible deactivation of active centers

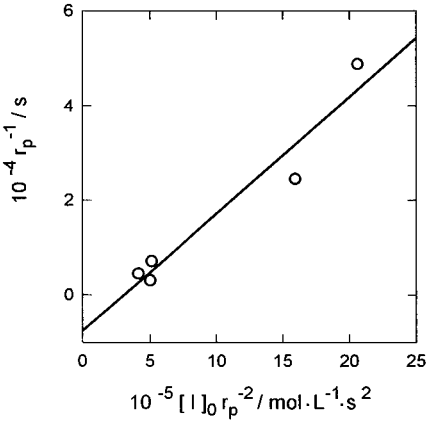

Figure 9. Determination of the propagation rate constants (k_p) and the aggregation equilibrium constant (K_a) in the polymerization of LA initiated with A_3. Plot of r_p^{-1} versus $[I]_0 r_p^{-2}$ (eq 12, $m = 2$). Polymerization conditions are are given in the caption for Figure 7.

by their aggregation. A similar phenomenon we already observed for the dialkylaluminum alkoxide/ϵ-caprolactone system.[38]

The pertinent kinetic scheme, in which the PLA chains grow exclusively with nonaggregated species, reads

$$m\,P_n^* \overset{K_a}{\rightleftharpoons} (P_n^*)_m$$

$$Pn^* + LA \overset{k_p}{\underset{k_d}{\rightleftharpoons}} P_{n+1}^*$$

$$[P_n^*] + m[(P_n^*)_m] = [I]_0 \qquad (11)$$

where $(P_n^*)_m$ and P_n^* denote the aggregated and nonaggregated active centers, respectively; K_a is the aggregation equilibrium constant; k_p and k_d are the *absolute* propagation and depropagation rate constants, respectively; and m is the degree of aggregation. Its solution, given in our earlier papers,[38] leads to eq 12, allowing the involved rate and equilibrium constants to be determined.

$$r_p^{\,1-m} = -mK_a k_p^{\,1-m} + k_p[I]_0 r_p^{\,-m} \qquad (12)$$

(where $r_p = \ln\{([LA]_0 - [LA]_{eq})/([LA] - [LA]_{eq})\}/t$ is a slope of the first-order kinetic plot (cf. Figure 7) determined for a given $[I]_0$).

After substituting $m = 2$, we have correlated the kinetic data from Figure 7 according to eq 12, i.e., in coordinates: r_p^{-1} versus $[I]_0 r_p^{-2}$. The resulting plot is shown in Figure 9. Its slope and intercept give $k_p = 8.2 \times 10^{-3}$ mol^{-1}·L·s^{-1} (for one alkoxide group in $Al(O^-...)_3$—cf. below) and $K_a = 94$ mol^{-1}·L, respectively.

A dependence of $\ln r_p$ against $\ln [I]_0$, reproduced on the basis of the kinetic scheme (11) with $m = 2$, i.e., with $\ln r_p$ calculated from the equation[38]

$$\ln r_p = \ln\{k_p(2K_a)^{-1/2}\} + \ln([I]_0)^{1/2} + \ln\{((8K_a[I]_0)^{-1} + 1)^{1/2} - (8K_{da}[I]_0)^{-1/2}\} \qquad (13)$$

(where $k_p = 8.2 \times 10^{-3}$ mol^{-1}·L·s^{-1} and $K_a = 94$ mol^{-1}·L, as determined above), is slightly curved but fits the experimental points almost perfectly (solid line in Figure 8). This curvature is related to a change of the molar fraction of the reactive, nonaggregated species

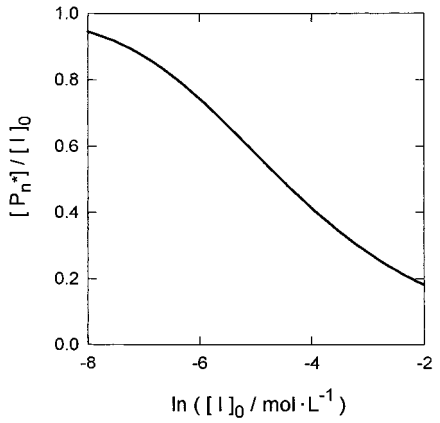

Figure 10. Dependence of the molar fraction of the nonaggregated active centers on the total concentration of active centers computed on the basis of the kinetic scheme (11), assuming $m = 2$ and $K_a = 94$ mol^{-1}·L ($[P_n^*] = r_p/k_p = (2K_a)^{-1/2}([I]_0)^{1/2}\{((8K_a[I]_0)^{-1} + 1)^{1/2} - (8K_{da}[I]_0)^{-1/2}\}$, from eq 13).

($[P_n^*]/[I]_0$) with initiator concentration in the feed ($[I]_0$) (Figure 10). For example, in agreement with the determined value of K_a, $[P_n^*]/[I]_0$ should increase from 0.20 to 0.86 for $[I]_0$ decreasing from 10^{-1} to 10^{-3} mol·L^{-1}.

Conclusions drawn in the present section need additional comment, since results of the studies of ϵ-caprolactone polymerization[26] might suggest that the tris(macroalkoxide) active centers are unable to aggregate at all.

Molecular weight measurements suggest that in the polymerization of LA initiated with Al(O^{i}Pr)$_3$ the growing PLA macromolecules form three-arm structures (cf. the present paper and refs 12, 14, and 16). Schematically

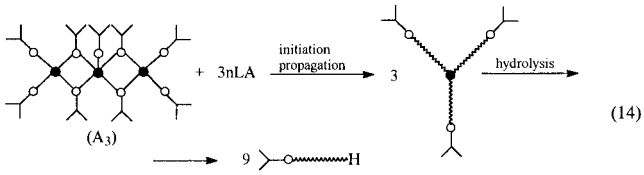

(14)

(where ○ and ● denote the oxygen and aluminum atoms, respectively; the isopropyl group; the PLA chain: $+OCH(CH_3)C(O)\frac{}{2n}$)

However, the structure of (^{i}PrO−PLA−O)$_3$Al in the scheme above is an oversimplification. Actually, the aluminum atoms in the living PLA species are, according to the ^{27}Al NMR spectra,[39] tetracoordinated. On the other hand in (^{i}PrO−PCL−O)$_3$Al, studied previously,[26,27] the hexacoordinated, nonaggregated species seems to dominate. The proposed structure assumes the intramolecular complexation of Al atoms by the acyl oxygen atom from the first PCL repeating units.

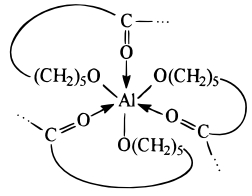

(living PCL)

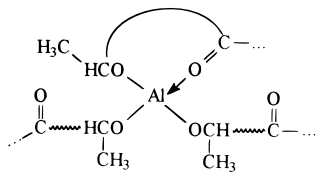

(living PLA)

Thus, for (^{i}PrO−PLA−O)$_3$Al we proposed a similar structure[39] but with only one acyl group−aluminum atom coordination bond (cf. PCL and PLA structures shown above), arguing that the complete saturation of the coordination shell (i.e., up to formation of the hexacoordinated Al atoms), via intramolecular complexation of Al atoms, is prohibited due to the steric hindrance created by the methyl group of the PLA repeating units.

Therefore, another kind of structure containing the tetracoordinated Al atoms could be a result of the reversible aggregation of the PLA tris(macroalkoxide)s, e.g.

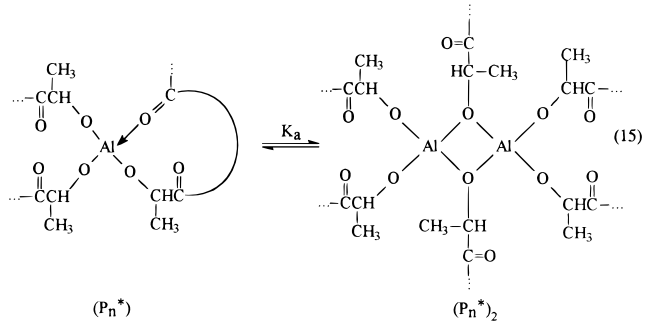

(15)

where only P_n^* is able to propagation and $(P_n^*)_2$ is unreactive, dormant species. This dimeric form is not preferred in the species based on repeating units derived from ϵCL, because the hexacoordination is energetically preferable. In LA polymerization, on the other hand, hexacoordination looks prohibited and both structures in eq 15 may coexist.

Equilibrium 15 could be responsible for the observed kinetic behavior, i.e., the fractional orders of propagation with respect to initiator (i.e., active centers). In the case of the ϵCL polymerization, the much stronger intramolecular complexation does not allow the intermolecular aggregates to be formed and eventually propagation is first-order in active centers.[26,40,41]

Acknowledgment. This work was realized within the research project no. 3 T09B 105 11 supported financially by the Polish Committee for Scientific Research (KBN).

References and Notes

(1) Kharash, G. B.; Sanchez-Riera, F.; Severson, D. K. Polymers of Lactid Acid. In *Plastics from Microbes*; Mobley, D. P., Ed.; Hanser Publishers: Munich, New York, 1994; p 93.
(2) Leenslag, J. W.; Pennings, A. J. *Makromol. Chem.* **1987**, *188*, 1809.
(3) Jamshidi, K.; Eberhard, R. C.; Hyon, S.-H.; Ikada, Y. *Polym. Prepr. (Am. Chem. Soc., Div. Polym. Chem.)* **1987**, *28* (1), 236.
(4) Duda, A.; Penczek, S. *Macromolecules* **1990**, *23*, 1636.
(5) Nijenhuis, A. J.; Grijpma, D. W.; Pennings, A. J. *Macromolecules* **1992**, *25*, 6419.
(6) Dahlman, J.; Rafler, G. *Acta Polym.* **1993**, *44*, 103.
(7) Zhang, X.; MacDonald, D. A.; Goosen, M. F. A.; McCauley, K. B. *J. Polym. Sci., Part A: Polym. Chem.* **1994**, *32*, 2965.
(8) Kricheldorf, H. R.; Kreiser-Saunders, I.; Boettcher, C. *Polymer* **1995**, *36*, 1253.
(9) In't Veld, P. J. A.; Velner, E. M.; van de Witte, P.; Hamhuis, J.; Dijkstra, P.J.; Feijen, J. *J. Polym. Sci., Part A: Polym. Chem.* **1997**, *35*, 219.
(10) Kowalski, A.; Duda, A.; Penczek, S. *Macromol. Rapid Commun.*, submitted for publication.
(11) Trofimoff, L.; Aida, T.; Inoue, S. *Chem. Lett.* **1987**, 991.
(12) Kricheldorf, H. R.; Berl, M.; Scharnagl, N. *Macromolecules* **1988**, *21*, 286.
(13) Kricheldorf, H. R.; Kreiser-Saunders, I. *Polymer* **1994**, *35*, 4175.
(14) Dubois, Ph.; Jacobs, C.; Jérôme, R.; Teyssiè, Ph. *Macromolecules* **1991**, *24*, 2266.

(15) Dubois, Ph.; Ropson, N.; Jérôme, R.; Teyssiè, Ph. *Macromolecules* **1996**, *29*, 1965.
(16) Degée, Ph.; Dubois, Ph.; Jérôme, R. *Macromol. Chem. Phys.* **1997**, *198*, 1973.
(17) Spassky, N.; Wisniewski, M.; Pluta, Ch.; LeBorgne, A. *Macromol. Chem. Phys.* **1996**, *197*, 2627.
(18) Montaudo, G.; Montaudo, M. S.; Puglisi, C.; Samperi, F.; Spassky, N.; Le Borgne, A.; Wisniewski, M. *Macromolecules* **1966**, *29*, 6461.
(19) Stevels, W. M.; Ankoné, M. J. K.; Dijkstra, P. J.; Feijen, J. *Macromolecules* **1996**, *29*, 6132.
(20) Bero, M.; Kasperczyk, J.; Jedlinski, Z. J. *Makromol. Chem.* **1990**, *191*, 2287.
(21) Bero, M.; Kasperczyk, J.; Adamus, G. *Makromol. Chem.* **1993**, *194*, 907.
(22) Kasperczyk, J. E. *Macromolecules* **1995**, *28*, 3937.
(23) Baran, J.; Duda, A.; Kowalski, A.; Szymanski, R.; Penczek, S. *Macromol. Rapid Commun.* **1997**, *18*, 325.
(24) Baran, J.; Duda, A.; Kowalski, A.; Szymanski, R.; Penczek, S. *Macromol. Symp.* **1997**, *123*, 93.
(25) Duda, A.; Penczek, S. *Macromol. Rapid Commun.* **1995**, *16*, 67.
(26) Duda, A.; Penczek, S. *Macromolecules* **1995**, *28*, 5981.
(27) Ropson, N.; Dubois, Ph.; Jérôme, R.; Teyssiè, Ph. *Macromolecules* **1995**, *28*, 7589.
(28) Bradley, D. C.; Mehrothra, R. C.; Gaur, D. P. *Metal Alkoxides* Academic Press: London, 1978; pp 74, 122.
(29) Shiner, V. J.; Whittaker, D. *J. Am. Chem. Soc.* **1969**, *91*, 394.
(30) Shiner, V. J.; Whittaker, D.; Fernandez, V. P. *J. Am. Chem. Soc.* **1963**, *85*, 2318.
(31) Oliver, J.G.; Phillips, P.K.; Worrall, I. J. *J. Inorg. Nucl. Chem.* **1969**, *31*, 1609.
(32) Kleinschmidt, D. C.; Shiner, V. J.; Whittaker, D. *J. Org. Chem.* **1973**, *38*, 3384.
(33) Duda, A.; Florjanczyk, Z.; Hofman, A.; Slomkowski, S.; Penczek, S. *Macromolecules* **1990**, *23*, 1640.
(34) Ronda, J. C.; Serra, A.; Matencón, A.; Cádiz, V. *J. Macromol. Sci.-Pure Appl. Chem.* **1995**, *A32*, 537.
(35) Penczek, S.; Kubisa, P.; Szymanski, R. *Makromol. Chem. Rapid Commun.* **1990**,*12*, 77.
(36) Beste, L. F.; Hall, H. K. *J. Phys. Chem.* **1964**, *68*, 269.
(37) Byrne, G.; Hindmarsh, A. EPISODE: An experimental package for the integration of systems of ordinary differential kinetic equations with bonded Jacobians. Lawrence Livermore National Laboratory report UCID-30132; Lawrence Livermore National Laboratory: Livermore, CA, April 1976.
(38) Duda, A.; Penczek, S. *Macromol. Rapid Commun.* **1994**, *15*, 559.
(39) Penczek, S.; Duda, A. *Macromol. Symp.* **1996**, *107*, 1.
(40) Ouhadi, T.; Stevens, Ch.; Teyssiè, Ph. *Makromol. Chem., Suppl.* **1975**, *1*, 191.
(41) Vion, J.-M.; Jérôme, R.; Teyssiè, Ph.; Aubin, M.; Prud'homme, R. E. *Macromolecules* **1986**, *19*, 1828.

MA971737K